AAPS PharmSci 2000; 2 (1) article 2 (http://www.aapspharmsci.org).

Molecular Modeling of G-protein Coupled Receptor Kinase 2: Docking and Biochemical Evaluation of Inhibitors

Submitted: August 20, 1999; Accepted: February 5, 2000; Published: February 21, 2000

Matthias U. Kassack[1,5], Petra Högger[2], Daniel A. Gschwend[3], Kimihiko Kameyama[4], Tatsuya Haga[4], Richard C. Graul[1] and Wolfgang Sadée[1]

[1]Department of Biopharmaceutical Sciences and Pharmaceutical Chemistry, University of California San Francisco, San Francisco, CA 94143-0446

[2]Institute of Pharmaceutical Chemistry, Westfälische Wilhelms Universität, 48149 Münster, Germany

[3]Department of Molecular and Cellular Biology, Harvard University, Cambridge, MA 02138

[4]Department of Neurochemistry, Faculty of Medicine, University of Tokyo, Tokyo, Japan

[5]Current Address: Pharmaceutical Institute, University of Bonn, An der Immenburg 4, 53121

ABSTRACT G-protein coupled receptor kinase 2 (GRK2) regulates the activity of many receptors. Because potent inhibitors of GRK2 are thus far limited to polyanionic compounds like heparin, we searched for new inhibitors with the aid of a molecular model of GRK2. We used the available crystal structure of cAMP dependent protein kinase (cAPK) as a template to construct a 3D homology model of GRK2. Known cAPK and GRK2 inhibitors were docked into the active sites of GRK2 and cAPK using DOCK v3.5. H8 docked into the hydrophobic pocket of the adenosine 5'-triphosphate (ATP) binding site of cAPK, consistent with its known competitive cAPK inhibition relative to ATP. Similarly, 3 of 4 known GRK2 inhibitors docked into the ATP binding pocket of GRK2 with good scores. Screening the *Fine Chemicals Directory* (FCD, containing the 3D structures of 13,000 compounds) for docking into the active sites of GRK2 identified H8 and the known GRK2 inhibitor trifluoperazine as candidates. Whereas H8 indeed inhibited light-dependent phosphorylation of rhodopsin by GRK2, but with low potency, 3 additional FCD compounds with promising GRK2 scores failed to inhibit GRK2. This result demonstrates limitations of the GRK2 model in predicting activity among diverse chemical structures. Docking suramin, an inhibitor of protein kinase C (not present in FCD) yielded a good fit into the ATP binding site of GRK2 over cAPK. Suramin did inhibit GRK2 with IC50 32 μM (pA_2 6.39 for competitive inhibition of ATP). Suramin congeners with fewer sulfonic acid residues (NF062, NF503 [IC50 14 μM]) or representing half of the suramin molecule (NF520) also inhibited GRK2 as predicted by docking. In conclusion, suramin and analogues are lead compounds in the development of more potent and selective inhibitors of GRK2.

***Corresponding author:** Matthias U. Kassack, Pharmaceutical Institute, University of Bonn, An der Immenburg 4, 53121;Telephone: +49-228-735240, Facsimile: +49-228-737929, E-mail: kassack@uni-bonn.de

KEYWORDS: Homology Modeling, Suramin, Suramin Analogues, Trifluoperazine

INTRODUCTION

G-protein coupled receptors (GPCRs) play an important role in signal transduction across the cell membrane. Upon agonist stimulation, GPCR activity is generally regulated by receptor phosphorylation[1], mediated mainly by 2 classes of kinases, ie, second messenger kinases (cAMP dependent protein kinase [cAPK], cGMP dependent protein kinase, protein kinase C, and Ca^{2+} /calmodulin dependent protein kinases)[2], and G-protein coupled receptor kinases (GRKs). The latter phosphorylate GPCRs only if the receptor is in an active or stimulated conformation[3]. Meanwhile, at least 7 GRK subtypes have been cloned[4,5] of which GRK2 (synonymous with βARK1, β-adrenergic receptor kinase 1) is extensively expressed in the central nervous system. GRK2 phosphorylates a variety of neurotransmitter receptors, including the β_2 adrenergic receptor[6]. Further known substrates of GRK2 are the α2 adrenergic receptor[7], muscarinic acetylcholine receptors[8,9], the d-opioid receptor[10], and rhodopsin, even though the latter is physiologically regulated by GRK1[11].

The pervasive role of GRK2 in GPCR regulation prompted us to initiate a search for selective inhibitors. So far, the polyanions, heparin and dextrane sulfate, are the most potent inhibitors (IC50 0.15 μM)[12]. However, they do not readily cross the cell membrane. In order to study the physiological impact of GRK2 on the regulation of GPCRs, a cell-permeable inhibitor would be useful. Knowledge of the 3D structure of the enzyme can be useful in the design of potent and selective inhibitors. The docking of compounds in large chemical databases into a molecular model of a target protein using the DOCK software package developed by Kuntz and collegues[16-19] has proven valuable as a screening procedure, providing insight into ligand-receptor interactions and suggesting possible lead compounds[20]. However, the crystal structure of GRK2 has yet to be reported. A large number of kinases share a highly conserved catalytic core, and the crystal structure of several kinases has already been reported. For example, the crystal

structure of the catalytic subunit of cAMP dependent protein kinase (cAPK) complexed with Mg adenosine 5'-triphosphate (ATP) and a peptide inhibitor has been resolved[13,14]. On the basis of high sequence identity between cAPK and the catalytic core of GRK2, we employed here the cAPK structure as a template for homology modeling of GRK2 in a fashion similar to that of Iino and Shibano[15]. Whereas Iino and Shibano applied their model to identify substrate recognition mechanisms of GRK2, we used our homology model as a means to better understand the molecular architecture of the active site and to guide the design of kinase inhibitors.

First, we compared the docking properties of known GRK2 and cAPK inhibitors using the molecular models of both enzymes. The molecular model of cAPK and the homology model of GRK2 served as screens for the best-fitting structures in a chemical databank (*Fine Chemicals Directory*). Subsequently, compounds identified with favorable docking parameters were also tested for their ability to inhibit GRK2 in a biochemical assay using rhodopsin phosphorylation[12]. We then tested known general inhibitors of protein kinases biochemically and by docking. The PKC inhibitor suramin selectively docked to and inhibited GRK2 over cAPK. This result prompted us to screen analogues of suramin, resulting in new lead compounds.

MATERIALS AND METHODS

Sequence Alignment of cAPK and GRK2 and Homology Modeling

The sequences of the catalytic subunit of cAPK (2CPKE.1, 350 amino acids) and GRK2 (ARK1_HUMAN, 689 amino acids) were aligned by a system of neural networks available by a mail server service (EMBL, Heidelberg, Germany, http://www.embl-heidelberg.de/Services/index.html)[21-23]. The alignment program does not insert gaps within predicted secondary structure elements (335 amino acids were aligned). Seven gaps were introduced into the sequence of cAPK. The atomic coordinates of the crystal structure of the catalytic subunit of cAPK complexed with MgATP and a peptide inhibitor were retrieved from the Brookhaven Protein Data Bank (2cpk, http://www.rcsb.org/pdb)[24]. The model of cAPK consists of catalytic residues 15 to 350[13].

For the construction of the GRK2 model, the 335 aligned amino acids were used. The gaps in the sequence of cAPK were not filled with the amino acid sequence of GRK2. The atomic coordinates of the amino acids in cAPK were applied to the corresponding amino acids in GRK2 using MIDAS Plus software[25] (available from http://www.sacs.ucsf.edu). The resulting model was energy minimized to convergence with Sybyl (Tripos Associates, St. Louis, MO) using a 3-stage protocol involving simplex, conjugate-gradient, and Powell minimization methods[26]. Calculations were performed on Silicon Graphics IRIS 4D/25 workstations (for further information see http://www.sgi.com/).

Docking of Potential Inhibitors of GRK2

Docking of potential inhibitors of GRK2 and cAPK was performed using the DOCK 3.5 software package[16-19]. Briefly, a molecular surface of the target site was created using the MS algorithm[27]. The target site on the GRK2 and cAPK models was chosen based on the contact region of cAPK and its protein inhibitor[14, 28]. The program SPHGEN[16] (available at http://www.sacs.ucsf.edu/) was used to create a negative image of the receptor site by filling the target region with overlapping spheres of varying sizes. The CHEMGRID program[18] (available at http://www.sacs.ucsf.edu/) generates grids for force-field interaction evaluation and was run using a grid resolution of 0.3 Å, a distance-dependent dielectric constant of 4r (where r is the interatomic separation), a nonbonded cutoff of 10 Å, and lose contact limits of 2.3 and 2.8 Å, respectively, for polar and nonpolar atoms. Hydrogens were added to the receptor in standard geometries.

The 89.2 version of *the Fine Chemicals Directory* (now called the *Available Chemicals Directory*[29]) was clustered by shape similarity using the method of Bemis and Kuntz[30]. The resulting database of 13,028 commercially available compounds was screened against GRK2 and cAPK with DOCK v3.5 using force-field score optimization with interpolation[19]. Two unfavorable contacts were tolerated in the docking, dislim was set to 1.5, ligand bin size and overlap were set to 0.1 and 0.1, and receptor bin size and overlap were set to 0.3 and 0.1; an average of 1,700 configurations were thus analyzed for each putative ligand.

Conformational Analysis and Docking of Known GRK2 and cAPK Inhibitors

Compounds were energy-minimized without electrostatics to convergence in Sybyl[26]. Conformations for each compound were generated using Sybyl's systematic search feature, retaining structures within 5 kcal/mol of the lowest energy conformation. Surviving conformations were docked to both GRK2 and cAPK using identical docking parameters as above.

Materials

γ-[^{33} P]-Adenosine triphosphate was purchased from DuPont NEN. Bovine cDNA of GRK2 (β-adrenergic receptor kinase 1) and a dominant-negative mutant of GRK2 (GRK2-K220W) were obtained from Dr. T. Haga (pEF-GRK2, pEF-GRK2-K220W)[31]. Bovine GRK2 shares 98% identity with human GRK2. The compounds

H7, IBMX, coralyne chloride, bicucullin methobromide, and suramin and the D-myo-inositolphosphates IP, IP2, and IP3 were purchased from Sigma Chemicals, St. Louis, MO. Nikkomycin Z was purchased from Calbiochem, La Jolla, CA. H8 was obtained from Seikagaku America Inc., Rockville, MD. The suramin analogues NF062, NF503, and NF520 were kindly provided by Dr. Peter Nickel, University of Bonn, Germany.

Cell Culture and Transfection of pEF-GRK2 and pEF-GRK2-K220W, a Dominant Negative Mutant

Human embryonic kidney cells (HEK293) were grown in Dulbecco's minimal essential medium (F12 50/50%) supplemented with 10% inactivated fetal calf serum at 37°C in 95% air and 5% CO_2. Twenty four hours prior to transfection, HEK293 cells were plated on 10-cm dishes (10^6 cells/dish). Cells were transiently transfected with 10 µg of pEF-GRK2 or pEF-GRK2-K220W per 10 cm dish using the calcium phosphate transfection method. After 48 hours, cells were scraped into 200-µl ice-cold lysis buffer per 10-cm dish (25 mM Tris-HCl pH 7.5, 5 mM EDTA, 0.1 mM phenylmethylsulfonylfluoride, 5 µg/mL pepstatin, 10 µg/mL leupeptin, and 10 µg/mL benzamidine). Cells were lysed using a dounce homogenizer (15 strokes), followed by centrifugation at 50,000*g* for 1 hour. The supernatant was used as source for GRK2 or dominant negative GRK2. Untransfected HEK293 cells were used as the control.

Detection of GRK2 Activity and Testing of Potential Inhibitors of GRK2

Rhodopsin served as substrate for GRK2. The preparation of urea-treated bovine rod outer segments (ROS) was performed as previously described[32] under dim red light. Urea-treated ROS showed no endogenous kinase activity, and rhodopsin accounted for the majority of proteins present, as assessed by Coomassie Blue staining of polyacrylamide gels.

Phosphorylation reactions employed urea-treated ROS (~200 pmol rhodopsin) and 10 µl supernatant of lysed transiently transfected HEK293 cells (or alternatively, 0.5 µl of GRK2 [2 µM, purified from Sf9 cells provided by Dr. T. Haga]) in 20 mM Tris HCl pH 7.5, 2 mM EDTA, 5 mM $MgCl_2$, and 100 µM γ-[^{33} P]-ATP (4440 cpm/fmol), prepared under red light and kept in the dark. Incubations were at 33°C in the presence of white light for 30 minutes, and were stopped by the addition of 1 mL ice-cold 100 mM sodium phosphate/5 mM EDTA buffer at pH 7.5. After centrifugation at 12,000*g* for 5 minutes, the pellet was resuspended in 30 µl SDS loading buffer (2% sodium dodecyl sulfate, 10% glycerol, 0.1 M dithiothreitol, 0.001% bromophenolblue in 0.08 M Tris HCl pH 6.8) and subjected to sodium dodecyl sulfate-polyacrylamide gel electrophoresis (SDS- PAGE) using a 10% homogenous polyacrylamide gel. After autoradiography, films were scanned using an Intas Imaging System (available from http://www.sacs.ucsf.edu/). Quantitative data were obtained with Gelscan 3D v2.1 (Marburg, Germany). To test potential inhibitors of GRK2, the compounds were added to the phosphorylation mixture at a final concentration of 100 µM unless otherwise stated. IC50 values were calculated using GraphPad Prizm Software v2.01.

RESULTS

Homology Model of GRK2 Based on cAPK

The sequence alignment of GRK2 with the catalytic subunit of cAPK (amino acids 15 to 350) yielded a residue identity of 31%. The aligned amino acids of GRK2 comprise residues 163 to 524, representing the catalytic domain of GRK2 (**Figure 1**). The amino- and carboxy-termini of GRK2 show no significant homology with cAPK[6] and were omitted from the GRK2 model. Several small gaps in the alignment of GRK2 with cAPK were located within exterior loops of the resolved cAPK structure, suggesting that their omission would not lead to serious distortion of the overall tertiary structure of GRK2. Thus, a total of 335 amino acids were used for the construction of the GRK2 model. Figure 2 shows an energy minimized, 3D molecular model of GRK2 (Figures **2A**, **2B**, **2C** [static images]) in comparison to cAPK (**Figure 2A** [static image]). The backbones of the 2 models are similar because of the introduction of several small gaps in the alignment of GRK2 with cAPK. Differences between GRK2 and cAPK are mainly prevalent in the side chains of the amide backbone leading to a different docking of compounds, ie., H8 (**Figure 2A** [static image]).

The tertiary structures of cAPK and the GRK2 model consist of 2 lobes, one large and the other small, embracing a central cleft for the binding of MgATP and substrate. The homology of GRK2 with cAPK is significantly larger in functional domains: the nucleotide binding motif as well as the catalytic loop are highly conserved (**Table 1**, and **Figure 2A** [static image]), as expected from the evolutionary relationships of serine/threonine protein kinases. ATP is deeply buried between the small and the large lobe; therefore, it is shielded from solvent (**Figure 2B** [static image]).

In cAPK, the adenine ring of ATP is anchored in a hydrophobic pocket with 2 additional H-bonds. The segment Met120 through Val123 plays a role in the recognition and anchoring of the adenine ring by hydrophobic interaction and hydrogen bonding, and it is the linker region between the small and large lobes[14]. The relevant amino acids are listed in **Table 1a**, along with the aligned amino acids of GRK2. Where residues differ between cAPK and GRK2, substitutions are conservative and can contribute to the hydrophobicity of the pocket or are capable of hydrogen bonding with the N6 amino

```
            15                  30                  45
cAPK        VKEFLAKAKEDFLKK WETPSQNTA-QLDQF DRIKTLGTGSFGRVM
GRK2        -QKFIESDKFTRFCQ WKNVELNIHLTMNDF SVHRIIGRGGFGEVY

            60                  75                  90
cAPK        LVKHKESGNHYAMKI LDKQKVVKLKQIEHT LNEKRILQAVNF---
GRK2        GCRKRDTGKMYAMKC LDKKRIKMKQGETLA LNERIMLSLVSTGDC

            105                 120                 135
cAPK        PFLVKLEFSFKDNSN LYMVMEYVAGGEMFS HLRRIGRFSEPHARF
GRK2        PFIVCMSYAFHTPDK LSFILDLMNGGDLHY HLSQHGVFSEADMRF

            150                 165                 180
cAPK        YAAQIVLTFEYLHSL DLIYRDLKPENLLID QQGYIQVTDFGFAKR
GRK2        YAAEIILGLEHMHNR FVVYRDLKPANILLD EHGHVRISDLGLACD

            195                 210                 225
cAPK        -VKGRTWTLCGTPEY LAPEIIL-SKGYNKA VDWWALGVLIYEMAA
GRK2        FSKKKPHASVGTHGY MAPEVLQKGVAYDSS ADWFSLGCMLFKLLR

            240                 255                 270
cAPK        GYPPFF---ADQPIQ IYEKIVSGKVRFPSH FSSDLKDLLRNLLQV
GRK2        GHSPFRQHKTKDKHE IDRMTLTMAVELPDS FSPELHSLLEGLLQR

            285                 300                 315
cAPK        DLTKRFGNLKNGVND IKNHKWFATTDWIAI YQRKVEAPFIPKF--
GRK2        DVNRRLGCLGRGAQE VKESPFFRSLDWQMV FLQRYPPPLIPPRGE

            330                 345                 360
cAPK        ---KGPGDTSNFDDY EEEEIRV-------- -----SINEKCGKEF
GRK2        VNAADAFDIGSFDEE DTKGIKLLDSDQELY RNFPLTISERWQQEV

            375
cAPK        TEF
GRK2        AET
```

Figure 1. Sequence alignment of GRK2 with the catalytic subunit of cAPK. The alignment starts with amino acid residue 15 of the cAPK catalytic subunit. The numbering includes the gaps introduced into the cAPK sequence. To determine the correct cAPK residue number, gaps have to be added.

group and N7 nitrogen of the adenine ring (Asp121 and Ser183 in GRK2). Similarly, the Glu127 residue in cAPK interacting with the 2'-hydroxy group of the ATP ribose ring[14] is substituted with an Asp residue in GRK2 (**Table 1b**). The invariant Lys72 residue present in all protein kinase catalytic domains, including GRK2, appears to be involved in the phospho-transfer reaction rather than in anchoring of ATP[33]. Glu91, also conserved in GRK2, stabilizes the anchoring of the α- and β-phosphates of ATP. The β-phosphate is further anchored by the backbone amides of the glycine-rich loop, which is highly conserved in GRK2 (**Table 1c**).

The catalytic loop is the most conserved region (**Table 1d**, and **Figure 2A** [static image]). All amino acids except one (Glu170, cAPK →Ala, GRK2) are invariant in cAPK and GRK2. Lys168, conserved in all Ser/Thr kinases, binds to the γ-phosphate, as demonstrated for cAPK complexed with an inhibitor[14]. In cAPK, the side chain of the invariant Asp166 is close to the serine/threonine of a substrate. One of the 2 magnesium

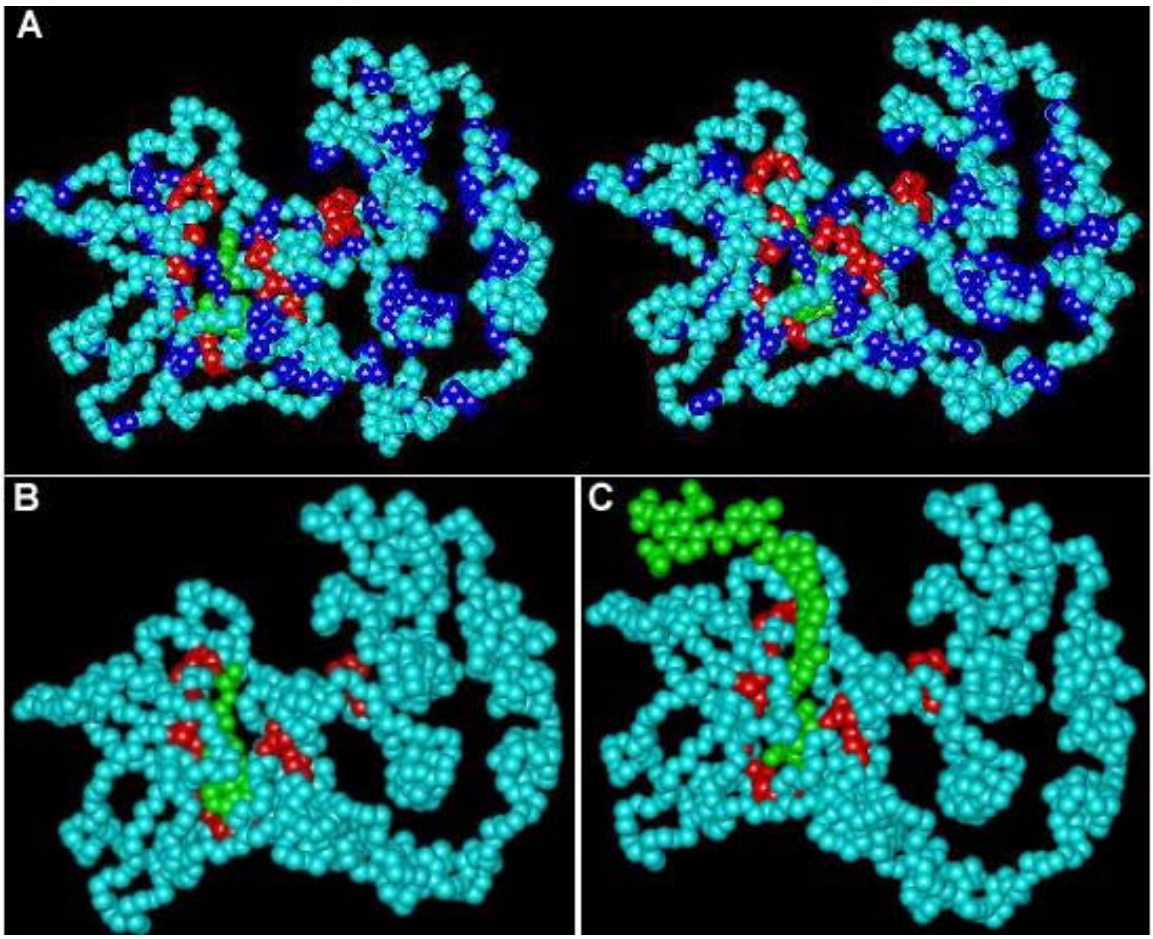

Figure 2. A) 3D molecular models of GRK2 (left) and cAPK (right) with H8 docked into the ATP binding site. Enzymes are displayed as backbone models. Invariant residues in GRK2 and cAPK are colored in blue. Invariant and conservative residues of the ATP binding site and the catalytic core are colored in red. The ligand H8 is colored in green. A: H8 fitted into the 3D molecular models of GRK2 (left) and cAPK (right). B: ATP fitted into GRK2. C: Suramin fitted into GRK2. To see the interactive Chime image, go to: http://itsa.ucsf.edu/~wsadee/grk/figure-2a.html; **B)** ATP fitted into the 3D molecular model of GRK2 (backbone model). Invariant and conservative residues of the ATP binding site and the catalytic core are colored in red. The ligand ATP is colored in green. To see the interactive Chime image, go to: http://itsa.ucsf.edu/~wsadee/grk/figure-2b.html; **C)** Suramin fitted into the 3D molecular model of GRK2 (backbone model). Invariant and conservative residues of the ATP binding site and the catalytic core are colored in red. The ligand suramin is colored in green. To see the interactive Chime image, go to: http://itsa.ucsf.edu/~wsadee/grk/figure-2c.html

ions in the cAPK crystal structure is coordinated by the oxygens of the β- and γ-phosphate of ATP and by the invariant Asp184. The second magnesium ion coordinates with the α- and γ-phosphates and the invariant Asn171. Thus, only 2 invariant residues from the large lobe contribute to the binding of the phosphates of ATP: Asn171 and Asp184. Mainly, the nucleotide binding motif is contained in the small lobe (glycine rich loop, Lys72, Glu91).

Docking of Compounds Into GRK2

Docking ATP into the GRK2 model yielded the expected good score (the more negative the value, the better the fit) with a fit close to the proposed ATP binding pocket (**Table 2B** and **Figure 2B** [static image]), indicating that the model is adequate for identifying the predicted ATP site. Minor deviations from the expected orientation may be the result of ommitting the Mg^{2+} ions associated with ATP in the active site because they could not be readily incorporated into the docking procedure. To identify a putative binding site for inhibitors, we first docked the

Table 1. Comparison of amino acids of cAPK and GRK2 involved in recognizing and anchoring of a) adenine ring, b) ribose, c) phosphates of ATP, and d) amino acids involved in the catalytic loop.

		cAPK	GRK2	
a)	Adenine Ring			
	Hydrophobic Pocket	Leu 49	Ile	conservative
		Val 57	Val	**invariant**
		Ala 70	Ala	**invariant**
		Met 120	Leu	conservative
		Tyr 122	Leu	conservative
		Val 123	Met	conservative
		Leu 173	Leu	**invariant**
	H-Bond: N6 Amino Group	Glu 121	Asp	conservative
	H-Bond: N7 Nitrogen	Thr 183	Ser	conservative
b)	Ribose 2' Hydroxy Group	Glu 127	Asp	conservative
c)	Alpha, Beta Phosphates	Lys 72	Lys	**invariant**
		Glu 91	Glu	**invariant**
	Beta Phosphate	Gly 50	Gly	**invariant**
		Thr 51	Arg	-
		Gly 52	Gly	**invariant**
		Ser 53	Gly	-
		Phe 54	Phe	**invariant**
		Gly 55	Gly	**invariant**
d)	Catalytic Loop	Tyr 164	Tyr	**invariant**
		Arg 165	Arg	**invariant**
		Asp 166	Asp	**invariant**
		Leu 167	Leu	**invariant**
		Lys 168	Lys	**invariant**
		Pro 169	Pro	**invariant**
		Glu 170	Ala	-
		Asn 171	Asn	**invariant**
		Asp 184	Asp	**invariant**

kinase inhibitor H8 into the model of cAPK and GRK2 (**Figure 2A** [static image]). Although H8 is a known and relatively selective cAPK inhibitor[34], its activity against GRK2 was unknown. In cAPK, the isoquinoline ring of H8 is preferentially docked into the hydrophobic binding pocket for the adenine ring of ATP (**Figure 2A** left [static image]), thereby possibly accounting for the competitive (with respect to ATP) inhibitory effect of H8 on cAPK[34]. For GRK2, H8 docked into the same pocket but with a slightly different rotation, yielding a slightly lower docking score than with cAPK (**Table 2**). H8 is indeed a weak inhibitor of GRK2 (**Table 2**) suggesting the hydrophobic ATP binding pocket as a putative target for GRK2 inhibitors. To test this hypothesis further, several known GRK2 inhibitors with published IC50 values[12] were also docked into the GRK2 and cAPK models. Although none of these known inhibitors were highly potent or selective (**Table 2A**), they docked into or close to the ATP binding pocket, except pyridoxal phosphate and tamoxifen, for which the binding pocket in GRK2 was less well defined. The docking scores and the inhibitory potency of the known GRK2 inhibitors did not correlate (**Table 2A**). Nevertheless, because most known inhibitors docked into the hydrophobic ATP binding pocket, these results support the potential relevance of this pocket as a putative target in the search of new inhibitors.

Subsequently, we screened a database containing 13,028 defined structures (FCD) by docking each into the GRK2 model. For the first screen, 1,000 structures were selected on the basis of their docking scores for GRK2. The same compounds were also docked into the molecular model of cAPK. To reduce the number of potential inhibitors identified by the docking screen, additional selection criteria included similar or superior scores for GRK2 over cAPK, in order to identify GRK2-selective inhibitors. Only compounds that scored well and had a favorable fit into the central cleft of GRK2, close to the hydrophobic ATP binding pocket, were selected and subsequently tested as inhibitors of GRK2. **Table 2** shows the docking scores of these selected compounds for GRK2 and cAPK. Only H8 showed a slightly better score for cAPK than GRK2, but it was nevertheless tested further because it is a known cAPK inhibitor with unknown activity towards GRK2.

In general, docking of polyanionic compounds is expected to be biased toward more negative scores in the docking procedure used and were therefore excluded in most cases. Inositol-1, 4-bisphosphate (IP2) was among the highest scoring and selective compounds for GRK2 in the screened chemical database. Even though IP2 is highly charged, inositol phosphates were tested further because they are important second messengers of GPCR signaling and may play a role in receptor regulation. Inositol-1-monophosphate (IP) and inositol-1, 4, 5-triphosphate (IP3), not contained in the database, were also modeled and docked, yielding excellent scores as well, with selectivity for GRK2 over cAPK (**Table 2**). These inositol phosphates were included because of their biological relevance, whereas the excellent GRK2 scores were suspected to be biased.

Last, we docked the general inhibitor suramin into the model of GRK2. Suramin gave an excellent score, with selectivity for GRK2 over cAPK and a good fit into the central cleft of GRK2 (**Figure 2C** [static image]). Sura

Table 2. GRK2 and cAPK docking scores for selected compounds with a good fit into the central cleft of the GRK2 model and cAPK. The more negative values indicate the better score. Also provided are the IC50 values for inhibiting GRK2, determined in this study or elsewhere (12), and published IC50 values for cAPK where available. Compounds are divided into groups according to the indicated criteria.

Compound	GRK2 Score	GRK2 IC50 (μM)	cAPK Score	cAPK IC50 (μM)
A. Compounds selected from FCD matching all criteria				
Trifluoperazine	-34.7	35	-32.6	n.a.
H8	-32.1	100–200	-33.3	1.2 μM (34)
Coralyne	-46.1	>>100	-42.2	n.a.
Bicuculline	-39.5	>>100	-36.8	n.a.
Nikkomycin Z	-39.5	>>100	-30.5	n.a.
B.Compounds from FCD not matching all criteria				
ATP	-90.4	-	-59.6	-
IP3	-100.1	inactive at 1000	-44.0	n.a.*
IP2	-64.9	inactive at 1000	-28.7	n.a.
IP	-48.0	inactive at 1000	-25.2	n.a.
C. Known GRK2 inhibitors not in FCD used				
Tamoxifen	-26.8	40	-26.5	n.a.
Chlorpromazine	-31.7	43	-31.9	n.a.
Sangivamycine	-31.4	67	-33.3	n.a.
H7	-32.0	250	-36.4	3.0 μM (34)
Pyridoxal Phosph.	-55.6	900	-32.1	n.a.
D. General or suspected kinase inhibitors not in FCD				
Suramin	-50.5	32	-29.5	656 (40)
IBMX	-25.5	>>100	-24.9	n.a.

min is also charged, but it contains a large lipophilic central section that is likely to play a role in the docking scores. Moreover, the purine analogue IBMX(1-isobutyl-3-methyl xanthine) was docked as a suspected kinase inhibitor, but it gave a rather poor score at both cAPK and GRK2.

Biochemical Evaluation of Potential Inhibitors of GRK2

The GRK2 assay is based on phosphorylation of the photoreceptor rhodopsin by GRK2[11]. **Figure 3** shows the ^{33} P-labeled band of rhodopsin at ~30 kd (and of rhodopsin oligomers at higher molecular weight) in a typical phosphorylation assay, using the cytosolic fraction of HEK293 cells transfected with GRK2 constructs as an enzyme source. The phosphorylation of rhodopsin was light-dependent, as can be seen from the GRK2 controls determined under dark or light conditions (lanes 1 and 2). Similar results were obtained with GRK2 purified from Sf9 cells using a baculovirus expression system[9] (data not shown). Addition of the transfected dominant negative mutant of GRK2 (GRK2-K220W, using the same plasmid construct) failed to enhance labeling of the light-activated rhodopsin band at ~30 kd (lane 4), relative to GRK2 wild-type, showing that transfected GRK2 kinase activity was required. Supernatants taken from untransfected HEK293 cells show little GRK2-like activity (lane 3). The rhodopsin preparation itself contained no endogenous kinase activity (data not shown). These control experiments demonstrate that the rhodopsin assay using supernatants of HEK293 cells transfected with GRK2 indeed measured GRK2 activity, rather than other kinase activities. As expected, the known GRK2 inhibitor heparin inhibited GRK2 by 90% at 1 μM (**Figure 4**).

Several compounds are known inhibitors of GRK2, but these are neither highly selective nor potent. Their published IC50 values for inhibiting GRK2[12] are listed in **Table 2**, in comparison to their docking scores for GRK2 and cAPK. Trifluoperazine, chlorpromazine, and sangivamycine displayed intermediate activity as GRK2 inhibitors, paralleling their intermediate scores obtained from docking into the ATP binding pocket. Compound H7 is considerably more potent in inhibiting cAPK than GRK2, paralleling its docking scores against GRK2 (-32.0) and cAPK (-36.4) (**Table 2C**). The rather low potency of pyridoxal phosphate relative to its excellent docking score likely resulted from overestimation of the score because of the charged phosphate moiety. On the

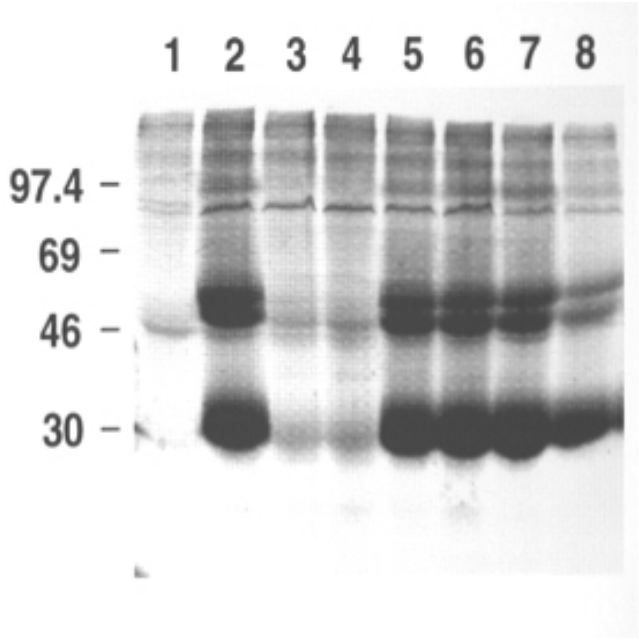

Figure 3. Autoradiogram of a typical GRK2 assay. Samples consisted of rhodopsin and supernatant of lysed HEK293 cells transiently transfected with GRK2, except lane 3, with supernatant of untransfected HEK293 cells, and lane 4, with supernatant of HEK293 cells transiently transfected with dominant negative GRK2. All samples were exposed to light except lane 1, which served as dark control. Lanes 5 to 8 contain the indicated compounds at 100 μM. Lane 5: bicuculline methobromide; lane 6: coralyne chloride; lane 7: nikkomycin Z; lane 8: H8. Phosphorylated rhodopsin appears as a strong band at ~30 kd as well as an apparent dimer. Each condition was repeated at least 3 times.

other hand, tamoxifen was relatively more potent while attaining a lesser docking score. This is probably related to the failure of this inhibitor to dock into the adenine binding pocket of GRK2. Although most known inhibitors docked into the ATP binding pocket with reasonable scores, there is no clear quantitative correlation between the GRK2 score and potency among compounds with different chemical structures.

We then tested several compounds identified by the docking screen of the chemical library. Compounds were selected if they showed an acceptable GRK2 score (<-30) similar to or in preference over cAPK and a good fit into the adenine binding pocket of GRK2. Among the selected compounds were trifluoperazine (previously shown to inhibit GRK2 with an IC50 of 35 μM[12] [**Table 2A**]), coralyne chloride, bicuculline methobromide, nikkomycin Z, and H8. Polyphosphates were excluded from the study because of their polyanionic structure, except for the inositol phosphates.

In contrast to trifluoperazine and H8 (weak GRK2 inhibitor), coralyne, bicucullin, and nikkomycin did not measurably inhibit GRK2 when added at 100 μM (**Figure 3** and **Figure 4**), even though they docked well into the central cleft of GRK2. Thus, searching the chemical library for inhibitors on the basis of the GRK2/cAPK resulted in several false positives, and we were unable to find a novel structure by this approach. Furthermore, none of the inositol phosphates (IP, IP2, IP3) showed any inhibition of GRK2 even at 1 mM (data not shown). As expected, the scores for these charged molecules were biased.

IBMX (1-isobutyl-3-methylxanthine), a known phosphodiesterase inhibitor and purine analogue, scored poorly against GRK2, and it was also tested for GRK2 inhibition (**Table 2**). Moreover, IBMX was included in this study because we had reported earlier that it inhibits a basal phosphorylation reaction of the μ-opioid receptor at 10 μM[35]. If GRK2 were involved in this phosphorylation reaction, we would have expected IBMX to inhibit GRK2 activity in our biochemical assay. However, IBMX failed to inhibit rhodopsin phosphorylation by GRK2 at 100 μM (**Figure 4**), and even at 250 μM, no inhibition of GRK2 occurred (data not shown). This finding suggests that a kinase other than GRK2 is likely to mediate the previously reported basal phosphorylation of the μ-opioid receptor[35]. Also, the poor docking score of IBMX is consistent with its failure to inhibit GRK2.

Several potential kinase inhibitors (not in the condensed FCD used) of unknown activity against GRK2 but with known inhibitory activity against other kinases were selected to test their ability to inhibit GRK2. The cAPK inhibitor H8 was found to inhibit GRK2 by 40% at 100 μM (**Figure 4**). When compared with H7 (IC50 = 250 μM)[12], H8 was only slightly more potent (IC50: 100-200 μM) reflecting their almost identical scores against GRK2. Because of its rather low potency, the IC50 value of H8 was not determined more precisely. The cAPK score of H8 is only slightly better than its GRK2 score, but H8 is a considerably more potent inhibitor of cAPK than of GRK2 (**Table 2**). Therefore, the GRK2 and cAPK scores did not correspond well with measured inhibitory potencies of H7 and H8.

Suramin, a known inhibitor of several different enzymes, including protein kinase C and (very weakly) cAPK[36], was also docked into our GRK2 homology model. Suramin occupies the entire length of the central cleft of GRK2 (**Figure 2C** [static image]) and attained a high docking score, with strong preference for GRK2 over cAPK (**Table 2**). Moreover, in our GRK2-rhodopsin assay, suramin was one of the most potent inhibitors among the tested compounds, with an IC50 of 32 ± 7 μM (**Table 2**, **Figure 4**). Suramin was shown to inhibit GRK2 in a competitive manner in regard to ATP. **Figure 5** shows the parallel right shift of the dose-response curve of ATP with increasing concentrations of suramin. Schild

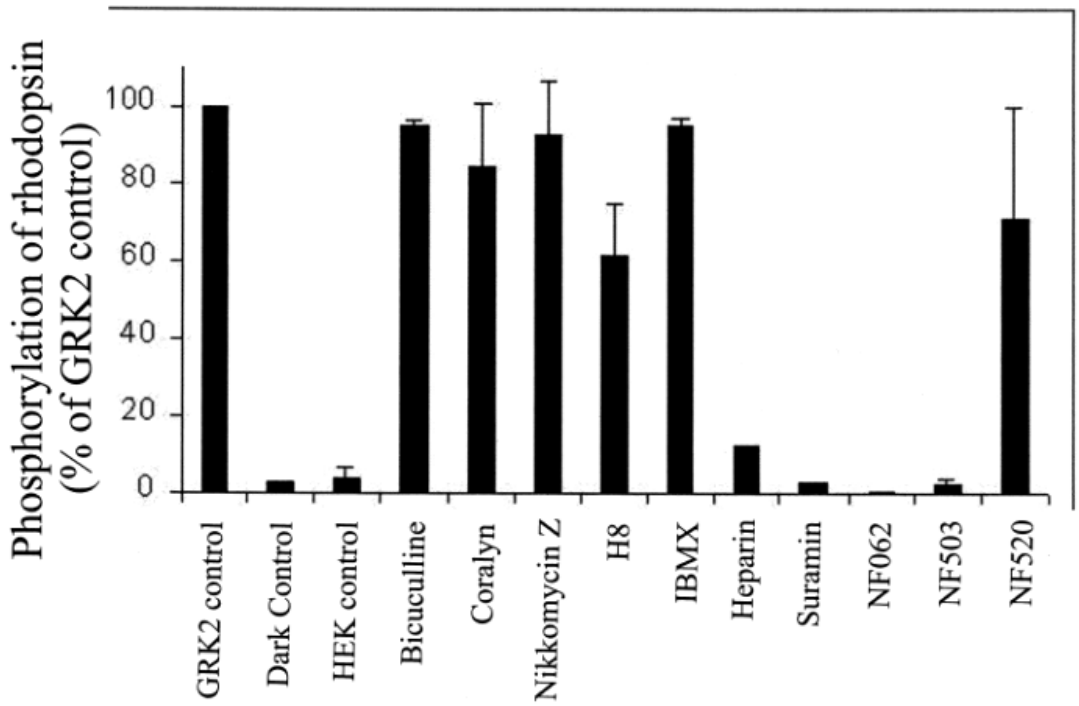

Figure 4. Inhibition of GRK2 mediated phosphorylation of rhodopsin. Concentration of the compounds was 100 μM, except for heparin (1 μM). All samples were exposed to light, except the bar labeled dark control. All samples contained supernatant of GRK2 transfected HEK293 cells or 0.5 μl of 2 μM GRK2 (purified from Sf9 cells), except for HEK control using supernatant of untransfected HEK293 cells. The data are the mean of 3 experiments, except for heparin (n = 1) and NF062 and NF503 (n = 2, instead of SD: mean deviation is shown).

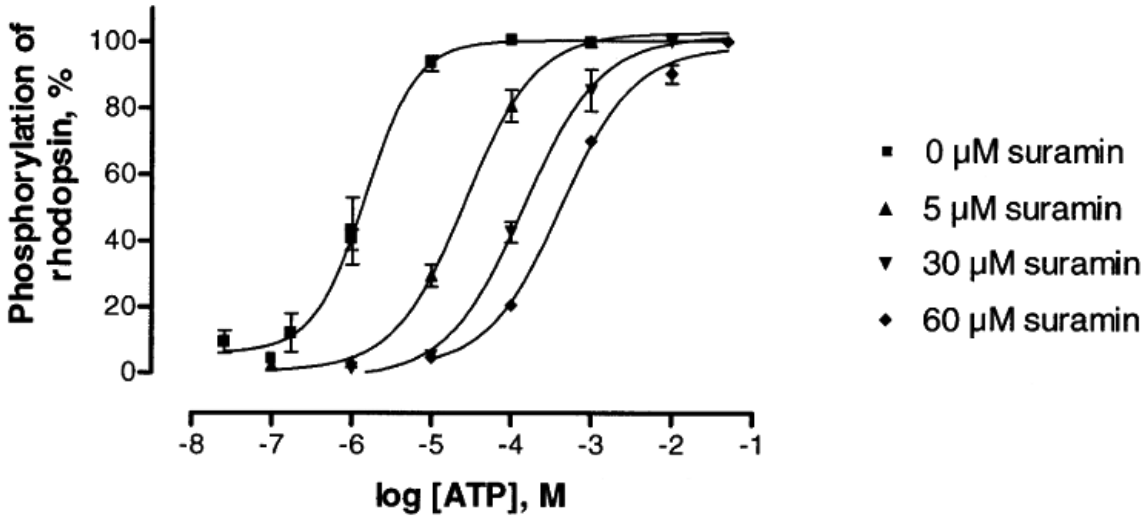

Figure 5. Competitive antagonism of GRK2 by suramin was shown by ATP-stimulated phosphorylation of rhodopsin in the absence and presence of 5, 30, and 60 μM of suramin, respectively. Each point represents the mean and SD of 3 independent experiments, except for 60 μM suramin (n = 2). 0 μM suramin: EC_{50} = 1.5 ± 0.1 μM; 5 μM suramin: EC_{50} = 26 ± 4 μM; 30 μM suramin: EC_{50} = 143 ± 25 μM; 60 μM suramin: EC_{50} = 419 ± 58 μM.

Table 3. Inhibition of GRK2 by suramin and related compounds.

Compound	IC50 (μM)	Structural formula
Suramin	32	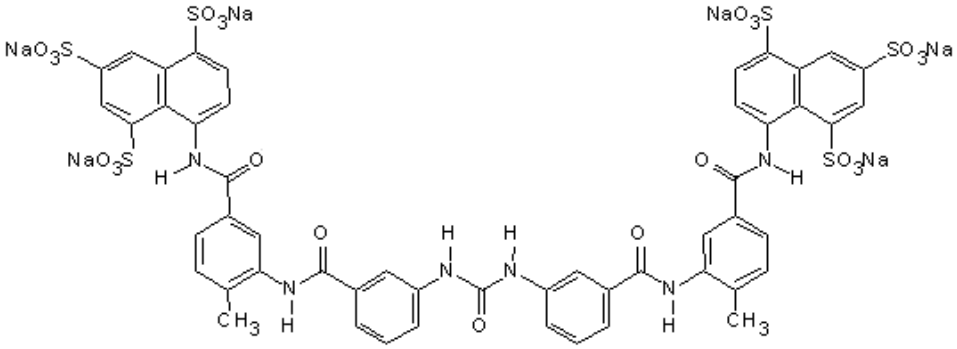
NF062	25	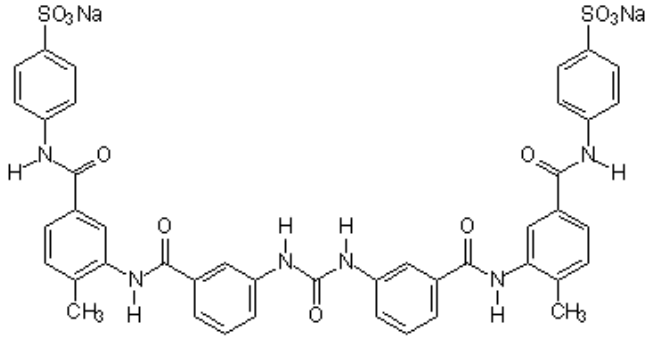
NF503	14	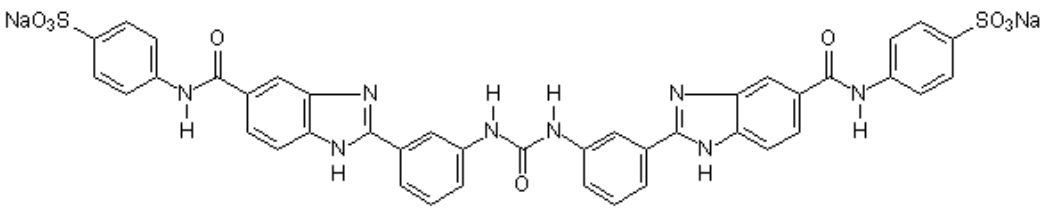
NF520	792	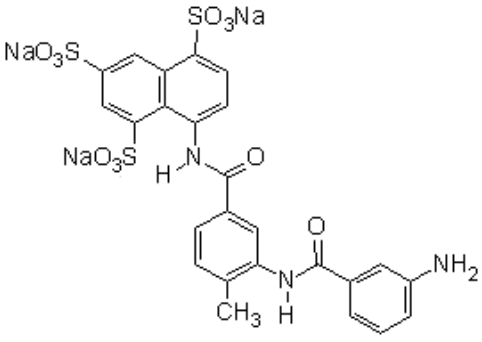

analysis yielded a linear regression, with a slope of 1.1 ± 0.1 and a pA_2 value of 6.39 ± 0.05.

Because the docking of suramin into our GRK2 homology model suggests that only a portion of the suramin molecule is bound into the central cleft of GRK2 (**Figure 2C** [static image]), we tested the precursor half-molecule NF520 for inhibition of GRK2 (**Table 3**). It indeed inhibited GRK2, but only at a high concentration (IC50 = 792 μM) (**Table 3**). Furthermore, we screened the suramin analogues NF062 and NF503 bearing only 2 instead of 6 sulfonic acid residues. Both compounds inhibited GRK2, with slightly lower IC50 values than suramin (**Table 3**). Thus, suramin analogues displayed inhibitory affinities in the low μM range

DISCUSSION

GRK2 plays an important role in the regulation of different G protein-coupled receptors[5]). So far, only polyanionic compounds like heparin are known potent inhibitors of GRK2. This prompted us to search for alternative potent and selective inhibitors of GRK2. The use of molecular modeling and docking of small compounds into the target sites of molecular models derived directly from resolved crystal structures has already proven valuable for discovering new ligands[20]. Moreover, this approach has also been successful for molecular models based on homology to a protein of known structure[38]. Our strategy was to construct a model of GRK2 based on high homology to the sequence of a kinase of known crystal structure, cAPK. Subsequently, we tested the homology model by docking ATP and already known inhibitors into the active site of GRK2 and its utility in screening and design of new inhibitors.

GRK2 is a homolog of cAPK, showing a high degree of identity in the nucleotide binding region and the catalytic loop (**Table 1**). The nucleotide binding domain holds ATP on one side of the cleft, whereas the catalytic loop embraces ATP from the other side. As found throughout the protein kinase family, residues Lys72, Glu91, Lys168, and Asp184 of cAPK are also invariant in GRK2[37] suggesting the same or a similar function for these residues in all kinases. This finding justified building a molecular model of GRK2 based on homology.

Because of the high homology in the nucleotide binding region and the catalytic loop between GRK2 and cAPK, the homology model of GRK2 retained a hydrophobic pocket within the central cleft accommodating the adenine ring of ATP (**Table 1**, **Figure 2B** [static image]) as well as being the preferred docking site for a number of test structures, eg, H8 (**Figure 2A** [static image]). As would be expected, ATP yielded a high score by fitting close to its predicted pocket. Subsequently, we docked known GRK2 inhibitors into the central cleft of the enzyme. Trifluoperazine, H7, chlorpromazine, and sangivamycine docked into the ATP binding pocket (**Table 2**). Although pyridoxal phosphate scores better than trifluoperazine, its IC50 is ~30-fold higher than that of trifluoperazine. A reason for this difference may be that pyridoxal phosphate does not show a preference for a particular pocket but that because of its anionic character it scores rather well. Electrostatic-ionic interactions are overestimated in the calculation of the docking scores because dehydration energies are not considered[20]. Tamoxifen, too, does not show a strong preference for a particular binding pocket and attains a poor score, yet it inhibits GRK2 with an IC50 of 40 μM. These results show that the homology model of GRK2 is able to identify the ATP binding pocket and to account for the inhibition of most of the docked known inhibitors of GRK2. Nevertheless, a quantitative correlation between the docking score and the inhibitory potency among diverse chemical structures could not be detected, and not all known inhibitors scored well. Currently, there are no GRK2 inhibitors of high potency available that fit tightly into the binding pocket, which makes it difficult to assess the general validity of the model. IBMX, scoring rather poorly, also did not inhibit GRK2, but we did not test additional negative controls.

A screen of the *Fine Chemicals Directory* based on an acceptable GRK2 score (<-30) with similar or poorer cAPK scores and with a good fit into the adenine binding pocket of GRK2 identified one (already known) GRK2 inhibitor, trifluoperazine (**Table 2A**). Furthermore, the cPKA inhibitor H8 scored well and was shown here to inhibit GKR2 weakly (**Table 2B**). Other compounds, even though scoring high, failed to inhibit GRK2 at 100 μM. This result demonstrates problems incurred with the screening of chemical libraries containing structures to which a single conformation has been assigned, docked to a homology model. Errors may also occur in our homology model of GRK2. Even though the model is adequate in identifying the ATP binding site, there may be errors due to the omission of amino acids in the model of GRK2. For example, amino acids in GRK2 corresponding to several small gaps in cAPK were omitted for the construction of the model. This omission may lead to a certain distortion of the binding sites of inhibitors, thus limiting the value of the homology model. Nevertheless, we showed that most of the known inhibitors docked into the ATP binding pocket. Thus, homology model and docking showed limited utility in discovering new chemical entities as GRK2 inhibitors, but they might be useful in guiding the further design of known lead compounds.

To extend our study to structurally distinct potential kinase inhibitors not contained in the *Fine Chemicals Directory* used, we tested suramin, a compound previously shown to inhibit protein kinase C[39] and, very weakly, cAPK[40]. Suramin was docked into the GRK2 model and attained a high GRK2 score with a favorable fit into the central cleft (**Figure 2C** [static image]), in preference to cAPK. Even though suramin is a hexasulfonic acid, its negative charges are separated by an extensive lipophilic middle portion that can be accommodated in the central cleft of GRK2. When tested in the rhodopsin phosphorylation assay, suramin was indeed shown to inhibit GRK2 in a competitive manner in regard to ATP (**Figure 5**). The pA_2 value of 6.39 (competing with ATP) reveals low micromolar affinity for the ATP binding site. Further, the considerably less favorable score for suramin docking into cAPK correlated with its reported lower inhibitory potency at cAPK[40]. The differences between docking of suramin to GRK2 and cAPK may be related to their different biochemical mechanisms: whereas cAPK commonly inserts a single phosphate onto Ser or Thr contained in a consensus site[28], GRK2 catalyzes the addition of multiple phosphates[4]. Thus, the sulfonated end of the suramin moiety docked inside the central cleft might stabilize binding to the enzyme in the same fashion as previously introduced

phosphates would assist in binding and further phosphorylation of a receptor substrate.

Even though suramin is known to enter cells by endocytosis[41], inhibitors with no or less negative charges are desirable for cell permeability. One of the sulfonated ends of suramin extended out of the central cleft of GRK2, suggesting that it does not contribute to the binding (**Figure 2c** [static image]). Therefore, we tested NF520, one half of the suramin molecule (**Table 3**). Indeed, NF520 was shown weakly to inhibit GRK2 (**Table 3**). Furthermore, the docking of suramin into our homology model of GRK2 suggests that compounds with a reduced number of sulfonic acid moieties but similar lipophilic aromatic residues might inhibit GRK2. We therefore tested compounds NF062 and NF503 (**Table 3**). The number of sulfonic acid groups can be reduced without loss of affinity. The disulfonic acid analogue NF062 (the negative charges are again separated by lipophilic aromatic residues as in suramin) and NF503, a zwitterionic compound, inhibited GRK2, with lower IC50 values than suramin (**Table 3**).

CONCLUSIONS

Whereas docking and subsequent screening of a chemical database showed a poor success rate, probably because of a simplified homology model of GRK2, we show here that the GRK2 homology model was useful in a first evaluation of putative inhibitors (suramin analogues) that dock into the ATP binding site of GRK2. Our results establish the suramin moiety as a promising lead in the design of GRK2 inhibitors that can penetrate the cell membrane. Because a large number of suramin analogues are available, a combination of selecting candidates by docking and biochemical testing might prove suitable for finding highly potent GRK2 inhibitors.

ACKNOWLEDGMENTS

This work was supported by Public Health NIH research grants, a General Medical Sciences grant (GM43102), a National Institute on Drug Abuse grant (DA04166), and the Japan Society for the Promotion of Science. The Deutsche Forschungsgemeinschaft (DFG) provided a fellowship for M.U.K. We acknowledge the assistance of Todd Ewing in clustering the database for docking. The facilities of the Computer Graphics Laboratory (NIH RR-1081, T. Ferrin, P.I.) were used for part of this project. We thank Tripos Associates for supplying Sybyl, and MDL Information Systems for providing the FCD structural database. The suramin analogues NF062, NF503, and NF520 were kindly provided by Dr. P. Nickel, University of Bonn, Germany.

REFERENCES

1. Lefkowitz RJ. G protein-coupled receptor kinases. Cell. 1993;74:409-412.

2. Hausdorff WP, Caron MG, Lefkowitz RJ. Turning off the signal: Desensitization of beta-adrenergic receptor function [published erratum appears in FASEB J 1990 Sep; 4(12):3049].FASEB J. 1990;4:2881-2889.

3. Palczewski K, Benovic JL. G-protein-coupled receptor kinases. Trends Biochem Sci. 1991;16:387-391.

4. Haga T, Haga K, Kameyama K. G protein-coupled receptor kinases.J Neurochem. 1994;63:400-412.

5. Pitcher JA, Freedman NJ, Lefkowitz RJ. G protein-coupled receptor kinases.Annu Rev Biochem. 1998;67:653-692.

6. Benovic JL, DeBlasi A, Stone WC, Caron MG, Lefkowitz RJ. Beta-adrenergic receptor kinase: Primary structure delineates a multigene family. Science. 1989;246:235-240.

7. Benovic JL, Regan JW, Matsui H, et al. Agonist-dependent phosphorylation of the alpha 2-adrenergic receptor by the beta-adrenergic receptor kinase. J Biol Chem. 1987;262:17251-17253.

8. Kwatra MM, Benovic JL, Caron MG, Lefkowitz RJ, Hosey MM. Phosphorylation of chick heart muscarinic cholinergic receptors by the beta-adrenergic receptor kinase. Biochemistry. 1989;28:4543-4547.

9. Haga K, Kameyama K, Haga T, Kikkawa U, Shiozaki K, Uchiyama H. Phosphorylation of human m1 muscarinic acetylcholine receptors by G protein-coupled receptor kinase 2 and protein kinase C. J Biol Chem. 1996;271:2776-2782.

10. Pei G, Kieffer BL, Lefkowitz RJ, Freedman NJ. Agonist-dependent phosphorylation of the mouse delta-opioid receptor: Involvement of G protein-coupled receptor kinases but not protein kinase C. Mol Pharmacol. 1995;48:173-177.

11. Benovic JL, Mayor FJ, Somers RL, Caron MG, Lefkowitz RJ. Light-dependent phosphorylation of rhodopsin by beta-adrenergic receptor kinase. Nature. 1986;321:869-872.

12. Benovic JL. Purification and characterization of beta-adrenergic receptor kinase. Methods Enzymol. 1991;200:351-362.

13. Knighton DR, Zheng JH, Ten Eyck LF, et al. Crystal structure of the catalytic subunit of cyclic adenosine monophosphate-dependent protein kinase [see comments]. Science. 1991;253:407-414.

14. Zheng J, Knighton DR, Ten Eyck LF, Karlsson R, Xuong N, Taylor SS, Sowadski JM. Crystal structure of the catalytic subunit of cAMP-dependent protein kinase complexed with MgATP and peptide inhibitor. Biochemistry. 1993;32:2154-2161.

15. Iino M, Shibano T. Substrate recognition mechanism of human beta-adrenergic receptor kinase 1 based on a 2-dimensional model structure. Drug Des Discov. 1996;14:145-155.

16. Kuntz ID, Blaney JM, Oatley SJ, Langridge R, Ferrin TE. A geometric approach to macromolecule-ligand interactions. J Mol Biol. 1982;161:269-288.

17. Shoichet BK, Bodian DL, Kuntz ID. Molecular docking using shape descriptors. J Comp Chem. 1992;13:380-397.

18. Meng EC, Shoichet BK, Kuntz ID. Automated docking with grid-based energy evaluation. J Comp Chem. 1992;13:505-524.

19. Gschwend DA, Kuntz ID. Orientational sampling and rigid-body minimization in molecular docking revisited: On-the-fly optimization and degeneracy removal. J Comput Aided Mol Des. 1996;10:123-132.

20. Kuntz ID. Structure-based strategies for drug design and discovery [see comments]. Science. 1992;257:1078-1082.

21. Sander C, Schneider R. Database of homology-derived protein structures and the structural meaning of sequence alignment. Proteins. 1991;9:56-68.

22. Rost B, Sander C. Improved prediction of protein secondary structure by use of sequence profiles and neural ne2rks. Proc Natl Acad Sci U S A. 1993;90:7558-7562.

23. Rost B, Sander C. Prediction of protein secondary structure at better than 70% accuracy. J Mol Biol. 1993;232:584-599.

24. Bernstein FC, Koetzle TF, Williams GJ, et al. The Protein Data Bank: A computer-based archival file for macromolecular structures. J Mol Biol. 1977;112:535-542.

25. Ferrin TE, Huang CC, Jarvis LE, Langridge R. The MIDAS Display System. J. Mol. Graph. 1988;6:13-27.

26. Sybyl v6.04a. Tripos Associates Inc., St. Louis, MO.

27. Connolly ML. Solvent-accessible surfaces of proteins and nucleic acids. Science. 1983;221:709-713.

28. Knighton DR, Zheng JH, Ten Eyck LF, Xuong NH, Taylor SS, Sowadski JM. Structure of a peptide inhibitor bound to the catalytic subunit of cyclic adenosine monophosphate-dependent protein kinase [see comments]. Science. 1991;253:414-420.

29. MDL Information Systems Inc., San Leandro, CA.

30. Bemis GW, Kuntz ID. A fast and efficient method for 2D and 3D molecular shape description. J Comput Aided Mol Des. 1992;6:607-628.

31. Kameyama K, Haga K, Haga T, Kontani K, Katada T, Fukada Y. Activation by G protein beta gamma subunits of beta-adrenergic and muscarinic receptor kinase. J Biol Chem. 1993;268:7753-7758.

32. Wilden U, Kuhn H. Light-dependent phosphorylation of rhodopsin: Number of phosphorylation sites. Biochemistry. 1982;21:3014-3022.

33. Carrera AC, Alexandrov K, Roberts TM. The conserved lysine of the catalytic domain of protein kinases is actively involved in the phosphotransfer reaction and not required for anchoring ATP. Proc Natl Acad Sci U S A. 1993;90:442-446.

34. Hidaka H, Inagaki M, Kawamoto S, Sasaki Y. Isoquinolinesulfonamides, novel and potent inhibitors of cyclic nucleotide dependent protein kinase and protein kinase C. Biochemistry. 1984;23:5036-5041.

35. Wang Z, Arden J, Sadee W. Basal phosphorylation of mu opioid receptor is agonist modulated and Cα2+-dependent. FEBS Lett. 1996;387:53-57.

36. Voogd TE, Vansterkenburg EL, Wilting J, Janssen LH. Recent research on the biological activity of suramin. Pharmacol Rev. 1993;45:177-203.

37. Hanks SK. Eukaryotic protein kinases. Curr Opin Struct Biol. 1991;1:369-383.

38. Ring CS, Sun E, McKerrow JH, Lee GK, Rosenthal PJ, Kuntz ID, Cohen FE. Structure-based inhibitor design by using protein models for the development of antiparasitic agents. Proc Natl Acad Sci U S A. 1993;90:3583-3587.

39. Hensey CE, Boscoboinik D, Azzi A. Suramin, an anti-cancer drug, inhibits protein kinase C and induces differentiation in neuroblastoma cell clone NB2A. FEBS Lett. 1989;258:156-158.

40. Mahoney CW, Azzi A, Huang KP. Effects of suramin, an anti-human immunodeficiency virus reverse transcriptase agent, on protein kinase C: Differential activation and inhibition of protein kinase C isozymes. J Biol Chem. 1990;265:5424-5428.

41. Baghdiguian S, Boudier JA, Boudier JL, Fantini J. Autoradiographic localization of tritiated suramin in polarized human colon adenocarcinoma cells. Cancer Lett. 1993;75:151-156.